



**POLarimetry with Cadmium telluride Array (POLCA) III**  
*Evaluation of Polarimetric capabilities of CdTe Array prototypes  
for hard X- and gamma ray astronomy*

Experiment No MI-966 Report

***Proposer:***

Ezio CAROLI, INAF/IASF-Bologna, Via Gobetti 101, Bologna, Italy

***Co-proposers:***

Rui Miguel CURADO DA SILVA, Dep. de Fisica, Universidade de Coimbra, Portugal

Stefano DEL SORDO, INAF/IASF-Palermo, Italy

Veijo HONKIMAKI, ESRF, Grenoble, France

John Buchan STEPHEN, INAF/IASF-Bologna, Italy

Natalia AURICCHIO, Dip. di Fisica, Università di Ferrara e INAF/IASF-Bologna, Italy

Alexandre TRINDADE, Dep. de Fisica, Universidade de Coimbra, Portugal

***Participants to beam tests:***

Ezio Caroli, INAF/IASF-Bologna, Italy

John Buchan Stephen, INAF/IASF-Bologna, Italy

Stefano del Sordo, INAF/IASF-Palermo, Italy

Natalia Auricchio, Dip. di Fisica, Università di Ferrara e INAF/IASF-Bologna, Italy

Alexandre Trindade, Dep. de Fisica, Universidade de Coimbra, Portugal

Rui Miguel Curado da Silva, Dep. de Fisica, Universidade de Coimbra, Portugal

Beamline: ID 15A  
Responsible: Dr. Veijo Honkimaki  
Shift Period: 5 May- 10 May 2009  
Number of shift: 12

**Table of contents**

1 Introduction ..... 3

2 Compton Scattering Polarimetry ..... 4

3 Inclined beam effects..... 4

    3.2 The synchrotron beamline optical system ..... 5

    3.3 The CdZnTe detection system..... 5

    3.4 The shaping and coincidence electronic subsystems..... 5

    3.5 The data acquisition unit..... 6

4 Results analysis ..... 7

5 Sensitivity to Beam Polarisation Degree..... 10

6 Pixel Vector Polarisation Vector Orientation Respect to Pixels ..... 10

7 Conclusion ..... 12

References ..... 12

## 1 INTRODUCTION

The experiment is an international collaboration project between the INAF/IASF–Bologna/Palermo, the University of Ferrara (I), the Dep. de Física da Universidade de Coimbra (PT) and the ESRF (F). The aim of this project is to optimize the design of CZT/CdTe pixel detectors for hard X and soft  $\gamma$ -ray astrophysics for performing high sensitivity polarimetric measurements together with spectroscopy, imaging and timing in the 100 keV–1 MeV range. In fact, polarimetry has been recognized as a very important observational parameter for high energy astrophysics ( $>100$  keV), as confirmed also by very recent and important results obtained from SPI/INTEGRAL data on the polarisation of the Crab pulsar [1]. Therefore, the capability of to perform accurate polarimetric measurement of high energy cosmic sources should really be included in proposals for future space missions. This idea was borne several years ago [2,3] with a view to implementation in a new generation of wide field telescope for high energy all sky survey and transient sources such as GRB's [4], but it has also become very appealing in the last three years in the development of a new telescope mission concept based on Laue focussing techniques for the next call for mission ideas in the ESA Cosmic Vision 225-2025 plan framework after a first submission in June 2006 [5]. Therefore, the possibility to realize the experiment described below will be critical in order to define the best design of CZT pixel detectors for both Laue lens focal plane and wide field monitors in order to obtain the best performance as Compton scattering hard X- and soft  $\gamma$ -ray polarimeters. As part of the design process, a sophisticated Monte Carlo simulation code based on the GEANT4 program has been developed [6], with which an extensive polarimetric study was performed in order to evaluate the response and performance of the detection plane to the type and level of linearly polarised radiation expected from different hard X and soft gamma ray astrophysical sources [7]. The present proposal represents the prosecution of a study that our collaboration have started in July 2002 with a first experiment (POLCA/MI-592) at the ERSF-ID 15 beamline. These tests have mainly allowed to compare and calibrate the simulation code with measurements results on a three small  $4\times 4$  pixel CdTe crystals that were tested under a  $\sim 100$  % polarised beam at 100,300,400 keV [8,9]. Encouraged by these results, we have developed a new larger CZT pixel detector with the aim to obtain more detailed information about the dependence of the polarisation modulation factor on incoming energy in the range 100-1000 keV and on the effect of Laue diffraction by Cu crystal on the photon polarisation status (POLCA II/MI-854, February 2007). The new proposal is based on a refurbished and improved version of the POLCA II detection system and is oriented to the study of some aspects related to scattering polarimetry with square pixel detector that was not the in the target of previous experiments: (a) Sensitivity of the detector to the level of the beam polarisation (i.e. the minimum percentage of photon polarisation that the detector is able to detect) as function of energy (100-1000 keV); (b) Modulation of the Q factor as a function of the azimuthal angle between the detector plane axis and the polarisation plane; (c) Systematic effects produced by the beam incident angle with respect to the detector plane. These results, compared with MC simulations, will allow us to be more confident in the evaluation of the achievable sensitivity to polarisation levels of high energy cosmic source emissions of instruments based on this technology and provide us with fundamental information to compare the achievable polarimetric performance with other detectors/instruments [10].

## 2 COMPTON SCATTERING POLARIMETRY

The polarimetric performance of a focal plane detector is based on the fundamental concepts associated with polarized Compton interactions. The Compton scattering of polarized photons generates a non uniformity in the angular distribution. After undergoing Compton scattering, the polarized photons' new direction depends on the orientation of its polarization vector before the interaction. If these polarized photons go through a new interaction inside the detector, the statistical distribution of the relative positions of the two interactions (double event) allows us to infer the degree and polarization direction of the incident radiation. The Klein-Nishina cross-section for linearly polarized photons gives us an azimuthal dependency for the scattered photons:

$$\frac{d\sigma}{d\Omega} = \frac{r_0^2}{2} \left(\frac{E'}{E}\right)^2 \left[ \frac{E'}{E} + \frac{E}{E'} - 2 \sin^2 \theta \cos^2 \varphi \right], \quad (1)$$

where  $r_0$  is the classical electron radius,  $E$  and  $E'$  are the energies of the incoming and outgoing photons respectively,  $\theta$  the Compton scatter angle and  $\varphi$  is the angle between the scattering plane (defined by the incoming and outgoing photon directions) and incident polarization plane (defined by the polarization vector and the direction of the incoming photon). As can be seen from (1), after fixing all other parameters the probability varies with the azimuthal angle  $\varphi$ . The cross-section reaches a maximum when  $\varphi = 90^\circ$ , that corresponds to the direction perpendicular to the initial polarization vector direction. However this relative difference is maximized for an angle  $\theta_M$ , dependent on the incident photon energy. For soft gamma and hard X-rays (100-1000 keV) the  $\theta_M$  value is about  $90^\circ$ .

The polarimetric performance of an instrument can be evaluated by analyzing the distribution of double events through the polarimetric modulation factor,  $Q$ . This is obtained by integrating the Compton polarimetric differential cross section formula given by (1) over the solid angles defined by the physical geometry of the detection plane and for a pixel detector can be written as:

$$Q = \frac{N_x - N_y}{N_x + N_y}. \quad (2)$$

Here we obtain  $Q$  through the orthogonal x- and y-axis directions defined over the detector plane, to a polarized beam whose electric vector points in the y direction.  $N_x$  and  $N_y$  are the number of counts in each of the orthogonal directions.

## 3 INCLINED BEAM EFFECTS

In general, it is assumed that the direction of the photons emitted by polarized sources is orthogonal with respect to the detection plane of the observation instrument. However, an off-axis source might generate a modulation of the Compton double event distribution that is not due to the incident beam polarization. As shown in Fig. 1, the incoming photons crossing the irradiated pixels surface will not be scattered uniformly inside these pixels. Preferentially they will be scattered closer or inside the first order pixels laying in the horizontal projection of the photon propagation direction. Consequently, the double event distribution will be affected by this asymmetry. This effect becomes more significant as the tilt angle  $\theta$  increases.

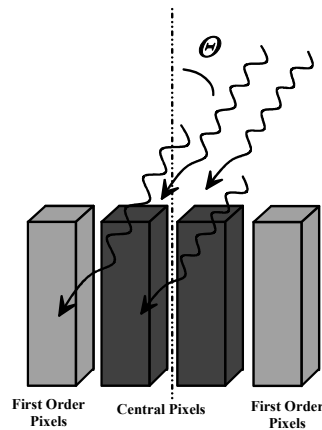


**Fig. 1.** Schematic view of central pixels irradiation by a polarised inclined beam at angle  $\theta$  with respect to the detector optical axis. In this case photons crossing the irradiated pixels surface will not be scattered uniformly inside this pixels. Preferentially they will be scattered closer or inside the first order pixels laying in the horizontal projection of the photon propagation direction. Consequently the double event distribution will be affected by this asymmetry.

### 3.1 Experimental Setup

In order to evaluate the CdZnTe pixel detector performance as scattering polarimeter for an off-axis polarized gamma-ray source, we tested a CZT polarimeter prototype under a  $\sim 100\%$  polarized beam at the ID (Insertion Device) 15A beamline of the ESRF (Fig. 2). The experimental system was composed of four functional subsystems: the synchrotron beamline optical system, the CdZnTe detection system, the shaping and coincidence electronic system and the control and data acquisition workstation.

### 3.2 The synchrotron beamline optical system

The ID 15A beamline optical system is composed of a set of diffracting crystals (Si(111), Si(311) or Si(331) ) that tune the energy of the monochromatic photon beam between 100 keV and up to 1 MeV, with a beam spot of about 500  $\mu\text{m}$  diameter and a linearly polarized component at the beam centre greater than 99 %.

### 3.3 The CdZnTe detection system

The detector employed in this experiment was based on an IMARAD 5 mm thick CdZnTe with segmented anodes to obtain a total of  $16 \times 16$  pixels, each with  $2.5 \times 2.5 \text{ mm}^2$  area. Due to limitations in our back-end electronics (only 128 channels available) only a continuous square matrix of  $11 \times 11$  pixels has been connected for a total sensitive area of  $\sim 7.5 \text{ cm}^2$ . The CdZnTe unit and the readout ASIC (Application-Specific Integrated Circuit) supplied by eV Products, PA, USA, were mounted on a supporting layer where were implemented the bias circuit and the connectors for the back-end electronics (Fig. 3). These devices sensitivity varies in function of the energy band selectable gain: 1.2 up to 7.2 mV/keV and a peaking time variable between 0.6 and 4  $\mu\text{s}$ . The detector system was mounted on a computer-controlled 3-axis and rotation positioning system provided by the ESRF.

### 3.4 The shaping and coincidence electronic subsystems

The signals were processed by a custom multiparametric system consisting of 128 independent channels with filters, coincidence logic and ADC (Analog-to-Digital Converter) units. When operating in coincidence mode, all signals exceeding the lower energy threshold occurring in the same coincidence time window (2  $\mu\text{s}$ ) are analyzed as generated by the same event. The typical irradiated pixel count rate was about  $10^4$  counts/s.

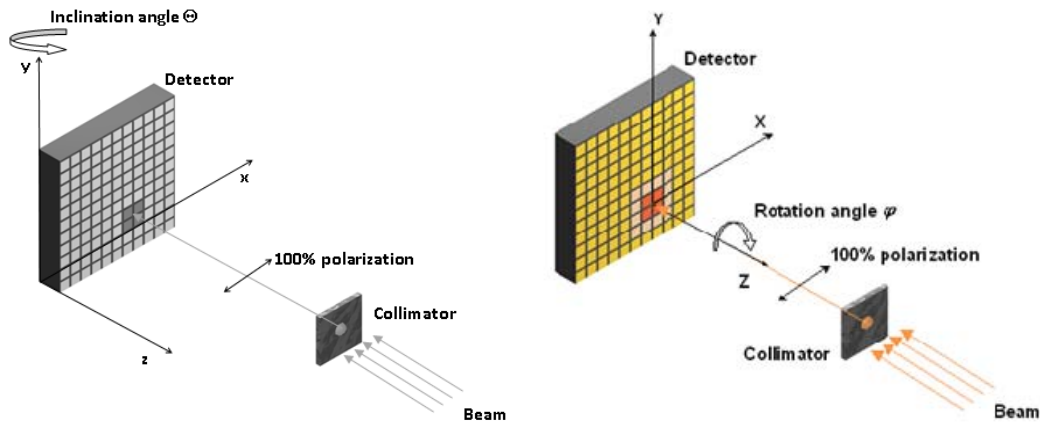


**Fig. 2.** (left) Schematic view of the experimental setup where the polarization vector is represented and the tilt angle  $\Theta$ . Measurements included polarization vector parallel both to  $x$  and  $y$  as well as  $\Theta$  rotation in  $x$  and  $y$ ; (right) Schematics of tests with polarization vector angle change. The beam polarization vector is represented at  $0^\circ$ , horizontally oriented relative to the experimental hutch reference frame. The detector was rotated around the beam axis ( $Z$  axis) by:  $5^\circ$ ,  $10^\circ$ ,  $20^\circ$ ,  $30^\circ$ ,  $40^\circ$  and  $45^\circ$  in order to simulate different polarization vector orientations during an observation of a cosmic ray source.

### 3.5 The data acquisition unit

This unit was based on a commercial data acquisition card PXI DAQ-6533 provided by National Instruments connected to a personal computer and controlled by a LABVIEW application. For each event we obtained information about the number of hits, the triggered pixels and the energy deposited in each hit. The recorded data is analysed off-line by an IDL (Interactive Data Language) s/w custom tool which allows the selection of single, double and multiple events (photons undergoing at least three interactions in the detection plane).

There are several effects that under certain conditions might introduce significant errors in the measurement of the modulation factor  $Q$ . Although the effects due to the quantization of possible scatter angles are always present in square pixelized detectors, laboratory non-polarized radioactive source measurements and Monte Carlo non-polarized beam simulations show that for CdTe and CZT the dominant source of error is the non-uniformity in pixel response, that may vary by more than 25% for a significant fraction of the pixels [11],[12].

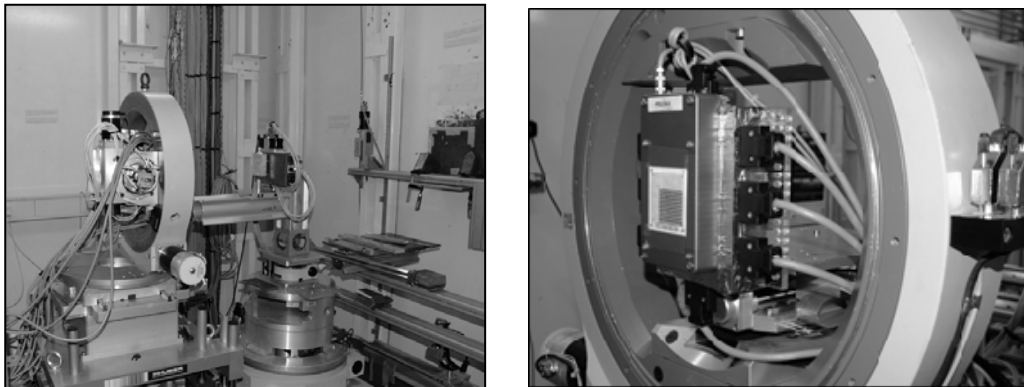


**Fig. 3.** Setup inside the experimental hutch of the ID15A beam line at the ESRF. The large ring rotates around directions parallel to the beam axis. In its center we placed the CZT pixelized prototype detector (zoom). The column where the ring was mounted could be rotated to the right or to the left in order to simulate the tilt of the incoming beam.

In order to minimise the systematic errors in the  $Q$  modulation factor evaluation we must consider two main effects: the non-uniformity of the detection efficiency of the pixels that compose the  $11 \times 11$  CdZnTe matrix and the alignment accuracy of the beam with respect to the irradiated pixel centre.

Before each measurement we performed a complete scan of all the detector pixels. The matrix obtained from the single events recorded in each pixel was used to correct the non uniformities inherent in the response of the detector pixels. We calculate the true double event counts  $N_{true}$  for each pixel by:

$$N_{true} = \frac{N_{pol}}{N_{non}} N_{max} \quad (3)$$

where  $N_{pol}$  is the number of double events detected (that depend on the beam polarization),  $N_{non}$  are the number of single events of the response map obtained when the pixel is directly irradiated and  $N_{max}$  is maximum value among all the matrix pixels  $N_{non}$  [2]. By applying this method to the pixels around the irradiated pixel, the error introduced by the non-uniformity of the detector matrix response is minimized thereby improving the precision of the modulation factor evaluation.

The photon beam was aligned in the x-y plane with respect to 4 central pixels (2×2), whose efficiency response was corrected as described above, by displacing the mechanical system until the weighted counts barycentre of these pixels aligned with the geometric centre of the 2×2 matrix. This allowed us to determine the offset of the beam with respect to the centre of the detector within 0.2 mm in both directions.

The centre of the target pixel was reached by moving the detector in both directions by steps equals to the pixel pitch ( $2.5 \pm 0.05$  mm) plus a fixed offset (1.125 mm). Taking into account that the pixel pitch is 2.5 mm and the beam spot diameter was set to 0.5 mm, a negligible systematic error on the  $Q$  factor evaluation is expected due to the alignment accuracy of the beam with respect to the target pixel centre. The irradiated pixel was chosen in order to optimise the uniformity of the response of the area defined by the pixels around the target. Previous tests showed that the pixel labelled as 186 (Fig. 4) was that which allowed best uniformity polarization measurements with a maximum pixel area around for Compton events to be detected. Since this pixel has only up to four order pixels along positive y, we considered only up to four order pixels in the remaining direction to avoid additional sources asymmetries. In practice, only a 9×9 matrix was taken into account all through the results presented herein.

Furthermore, taking into account the mechanical tolerance of both the detector mounting inside the shielding container (0.05 mm) and the container mounting on the ESRF roto/translator system (0.05 mm) we estimated an error within 5' in the perpendicularity between the detector plane and the beam impinging direction. As demonstrated in [11] and later by the presented results this error does not significantly affect the modulation factor evaluation.

After this procedure the detector central pixel was irradiated by the polarized beam forming different inclination angles with the optical detector axis: 0°, 0.5°, 1°, 1.5°, 2°, 3°, 4°, 5° and 10°. These measurements at different tilt angles were then repeated for different energies (200 keV, 300 keV, 400 keV and 511 keV) and polarization vector directions parallel to the detector plane axis:  $x$  and  $y$ . Then the modulation of the  $Q$  factor as a function of the angle  $\theta$  was calculated from the double event distributions obtained from each measurement.

## 4 RESULTS ANALYSIS

As can be seen in Figure 4, at 300 keV the beam inclination generates an asymmetric component in the double event distributions for all the hit relative distances, around the irradiated pixel, in the direction of the projection of the beam.

Since the effect of beam inclination projects along the positive x direction, the pixels to the right of the irradiated pixel show a higher number of detected double events, for a beam tilt of 10°. Figure 5 shows this asymmetry more explicitly by expressing the number of double

events as function of photon azimuthal scattering angle. Due to the beam inclination some of the photons irradiating the central pixel's surface cross these pixels without interacting with the material and penetrate adjacent pixels (first order pixels) and undergo a first interaction therein (Fig. 1). For a beam whose polarization vector lies orthogonally to the beam projection generated by its inclination, the contributions of polarization modulation and beam inclination are added and the distribution is evidently asymmetric. Obviously, for a beam whose polarization vector is parallel to the beam projection the two contributions are opposite and tend to cancel each other.

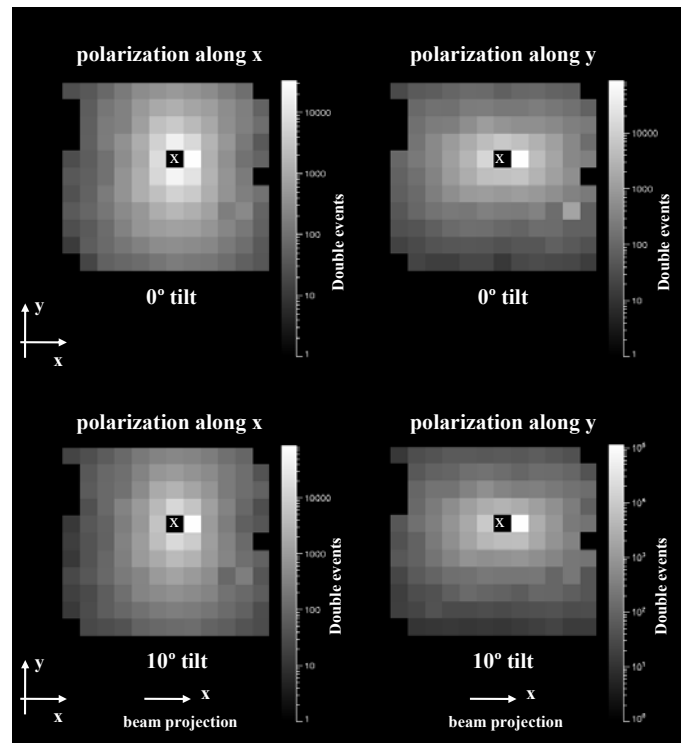


**Fig. 4.** Double event counts distribution maps obtained by irradiating CZT pixel number 186 (labeled x) with a  $\sim 100\%$  polarized 300 keV beam. The central pixel was irradiated orthogonally ( $0^\circ$ ) and at an angle  $\Theta = 10^\circ$ , with respect to the detector optical axis. Two pixels at the extreme right were off. In some rows there are 12 active pixels due to the fact that the readout electronics handle a total of 128 channels .

When calculating the  $Q$  modulation factor these asymmetry effects due to beam inclination on double event distributions are better understood. The experimental and simulated modulation factor obtained for this prototype as a function of the energy for an orthogonal beam is represented in Fig. 6. For energies higher than 550 keV, a secondary synchrotron beam (due to a gap in the beam collimator shield) was projected onto the CdZnTe active and passive surface area which generated fake single, double and multiple events, reducing the proportion of true double events recorded and consequently reducing the calculated  $Q$  factor. In the same figure is shown the measured modulation component produced by the non-uniformity of the response of pixelized matrix due to imperfections in the material. In Fig. 7 and Fig. 8 are plotted the  $Q$  factors as a function of the tilt angle. Up to  $2^\circ$  tilt angle the  $Q$  factor is not significantly affected by the beam inclination. However from  $3^\circ$  up to  $10^\circ$  tilt angles, the  $Q$  factor dramatically increases when polarization and inclination add their effects and decreases when these effects partially cancel each other. These results confirm previous simulation studies performed by a Monte Carlo simulation program based on GEANT4 [11]. Both experimental and simulation results show that during an observation period onboard a gamma-ray satellite, it is essential that polarized sources are no more than  $2^\circ$  off-axis in order that polarization measurements are not affected.

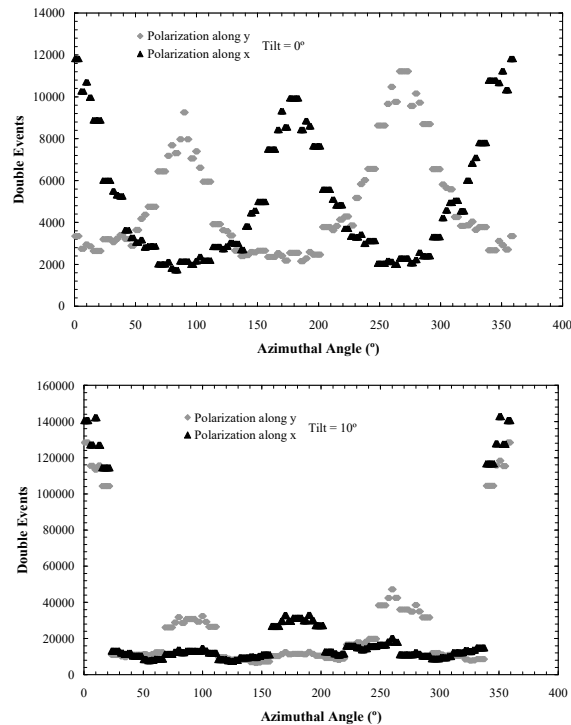


**Fig. 5.** Double events as a function of the scattering azimuthal angle obtained for a  $\sim 100\%$  polarized 300 keV beam along x and along y when (top) the beam is on-axis and when (bottom) the beam is off-axis by  $10^\circ$ . In the case of a tilted beam the horizontal projection of the photon propagation direction lays along positive x direction (azimuthal angle  $\sim 0^\circ$ ), that is in fact the angular direction for which significant number double events are recorded.

This study shows the importance of a pointing system with accuracy better than  $1^\circ$  for an instrument designed for polarimetry. This accuracy should be sufficient so that double event distributions can be read directly with no further need of correction methods. It must be pointed out that for a Laue lens optics the diffraction Bragg angle (i.e. the angle of impinging photons respect to the detector plane) is always much less than  $1^\circ$ . Furthermore, previous theoretical studies together with experimental work has confirmed that the polarization status of a beam is not changed after Laue diffraction at small angles ( $<1^\circ$ ) [13]-[15].

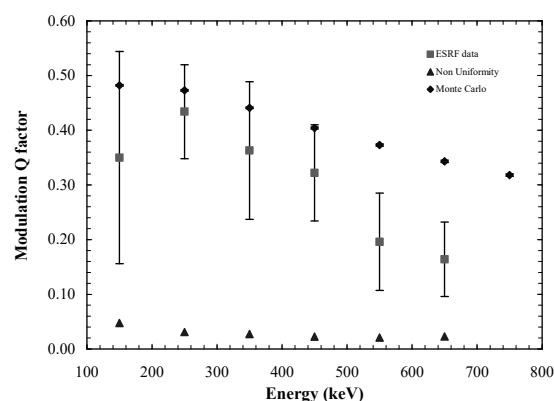


**Fig. 6.** The  $Q$  factor as function of the energy for a 5 mm CdZnTe prototype when irradiated by a monochromatic  $\sim 99\%$  polarized photon beam. Monte Carlo simulation obtained in similar conditions are shown for comparison. The modulation generated by the non-uniformity of matrix pixels response is also represented (triangle). The simulated residual modulation obtained for an unpolarized beam in the same energy range was lower than 0.01 [11].

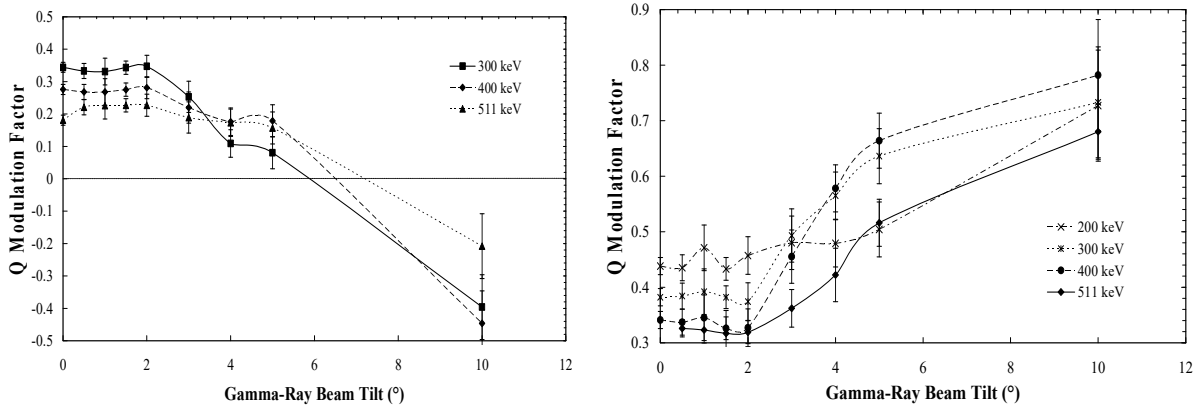


**Fig. 7.** (left)  $Q$  factor as a function of the tilt angle of the ESRF 100% polarized beam for several energies. In this case the polarization vector is parallel to x-axis; (right)  $Q$  factor as a function of the tilt angle of the ESRF 100% polarized beam for several energies. In this case the polarization vector is parallel to y-axis

## 5 SENSITIVITY TO BEAM POLARISATION DEGREE

After the correction procedures the CZT matrix prototype was irradiated with the polarized 400 keV monochromatic beam by centring it in an internal pixel. First we start with a polarization level of about 100%, afterwards other measurements were performed for 80%, 65%, and 50%. As already mentioned, as the polarization level was lowered the beam flux was lower and the observation time needed was exponentially longer. For polarization levels lower than 50% the time needed for each measurement was not compatible with the beam time available at the ESRF. Through the modulation obtained in the double event distribution around the irradiated pixel it was possible to calculate a modulation factor  $Q$  for each polarization level. Fig. 8 shows a linear relation between the polarization level of the beam and the measured  $Q$  factor – different from the  $Q$  factor of an instrument, which is the  $Q$  obtained for 100% polarized emission. At least, down to 50% this CZT prototype showed a good sensitivity to the degree of beam polarization. In future experiments we hope to have enough time available to go further down in polarization degree, down to the lowest polarization levels expected in the main gamma and X-ray celestial sources.

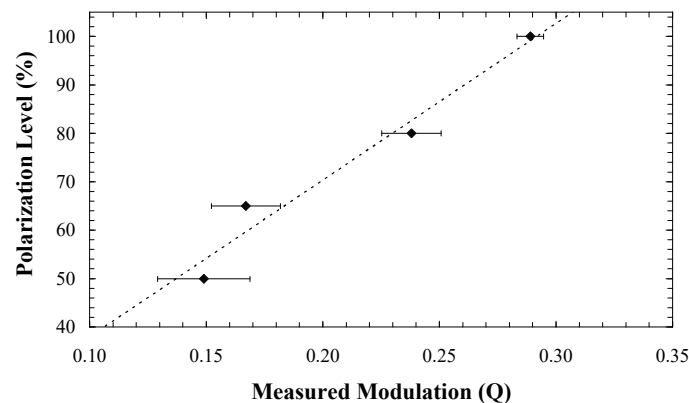


**Fig.8.** By varying the polarization of a 400 keV ESRF ID15 photon beam from 100% to 50%, a modulation  $Q$  factor was obtained by the analysis of the Compton event distributions generated in a CZT pixelized detector prototype. The results show a good linearity in the polarimetric response of the CZT prototype detector to the level of polarization of the gamma-ray beam.

## 6 PIXEL VECTOR POLARISATION VECTOR ORIENTATION RESPECT TO PIXELS

Another source of polarization measurement systematic effects arises from the discretization inherent to the size of the voxels of a pixelized polarimeter. This effect becomes very

important with square pixels when the polarization vector does not align with either of the two main axes of the pixelized matrix and when the double event distribution around a central pixel spreads only over a few pixels away from the central pixel. In order to study the accuracy of the polarization angle determination when the polarization angle is not parallel or perpendicular to the sides of the CZT matrix, the same setup was used. As before a central pixel was irradiated, however this time the support ring of the detector prototype was rotated by  $5^\circ$ ,  $10^\circ$ ,  $20^\circ$ ,  $30^\circ$ ,  $40^\circ$  and  $45^\circ$ . These measurements were performed for 100% polarized monochromatic beams at 300 keV and 511 keV. Fig. 9 Double events maps obtained for a set of 100% polarized beams by varying the polarization vector direction at:  $0^\circ$ ,  $10^\circ$ ,  $20^\circ$ ,  $30^\circ$ ,  $40^\circ$  and  $45^\circ$ . The 511 keV monochromatic beam irradiated the central pixel of the CZT prototype pixel matrix in black. Fig. 9 shows the double event distributions obtained for a 511 keV monochromatic beam with several polarization vector angles ranging from  $0^\circ$  to  $45^\circ$ . As can be seen for a polarization vector of  $0^\circ$  the double events are not  $360^\circ$  uniformly distributed around the irradiated pixel. A higher number of Compton photos were detected in the direction defined by top-center-bottom of the matrix (vertical direction inside the experimental hutch). This confirms the horizontal polarization inside the experimental hutch. When the CZT matrix is rotated  $0^\circ$ ,  $10^\circ$ ,  $20^\circ$ ,  $30^\circ$ ,  $40^\circ$  and  $45^\circ$  by the mechanical of Fig. 2 (right) the projection of the polarization vector in the detector surface is also rotated by the same amount. It is noticeable that the yellow regions of Fig. 2 maps, those that register more double events, rotate according to the polarization vector angle. It is possible to optimize the modulation Q factor by changing the amplitude of the radial bin of the double events considered in the Q factor calculation (Fig. 10).

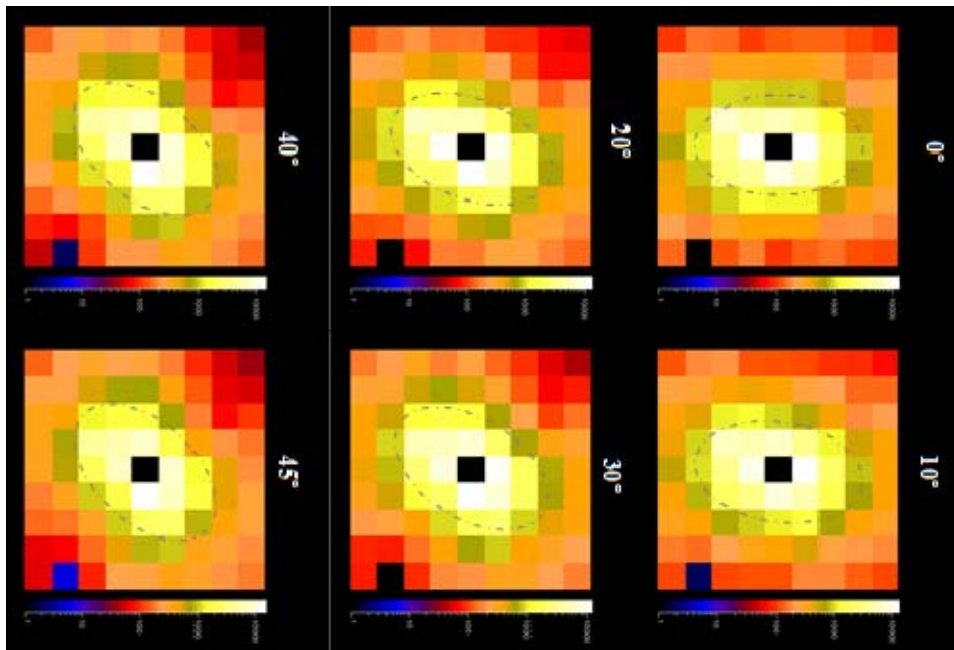


**Fig. 9.** Double events maps obtained for a 100% polarized beam by rotating the polarization vector angle,  $\phi$ , of:  $0^\circ$ ,  $10^\circ$ ,  $20^\circ$ ,  $30^\circ$ ,  $40^\circ$  and  $45^\circ$  with respect to the detector sides axis. The 511 keV monochromatic beam was directed to a CZT matrix central pixel, in black at the centre. A dashed ellipse was fitted to the double event distribution. Note that the major ellipse axis is oriented with the pixels that recorded more Compton photons. The minor axis is perpendicular and is aligned with the incoming beam polarization vector direction.

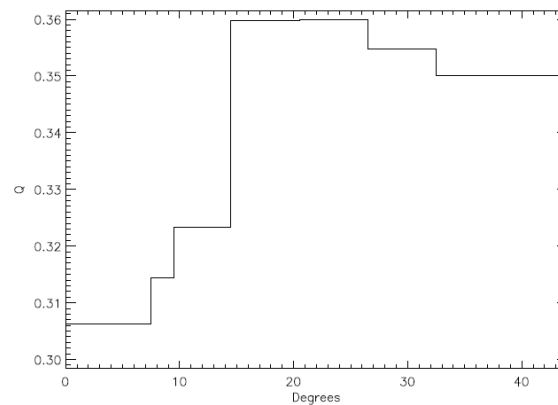


**Fig. 10.** Modulation  $Q$  factor as a function of the radial bin aperture angle for a fully polarized 300 keV gamma-ray beam and  $0^\circ$  polarization vector.

## 7 CONCLUSION

We showed that the beam inclination can give rise to significant changes of the modulation  $Q$  factor calculated for beam inclinations greater than  $2^\circ$ , confirming previous results obtained by MonteCarlo studies. This means that in the case of a focusing instrument whose focal plane detector is designed for polarimetric measurements, the inclination of the impinging photons respect to the detector axis shall fit within  $2^\circ$  inclination angle. This will allow a direct double event distribution analysis with no need of complex correction methods. However, in general the required pointing accuracy of a next Laue lens telescope should be better than  $1^\circ$ , therefore the polarimetric performance of the instruments will not be affected. Furthermore, This experiment showed that a CZT pixelized matrix is potentially able to discriminate a gamma-ray level of polarization lower than 50% (minimum useful polarization available at ESRF). Although square pixels introduce systematic effects on the modulation of double event distribution when irradiating a central pixel, it was also shown that through appropriate analysis tools and correction methods a  $9 \times 9$  planar squared pixelized matrix is able to measure polarized beam vector angles, ranging from  $0^\circ$  to  $45^\circ$  with respect to the CZT detector axes, within an angular range of a few degrees. Obviously, better performances are expected from higher pixelization level polarimeters than the  $9 \times 9$  pixel prototype, such as the focal plane detectors that are being projected for future gamma-ray telescope missions.

## References

1. A.J. Dean, et al., *Science*, 321, pp. 11-83 (2008)
2. E. Caroli, et al., *Nucl. Instr. and Meth. Section A*, 448, pp 525-530 (2000);
3. R. M. Curado da Silva, et al., *Experimental Astronomy*, 15, pp. 45-65 (2003).
4. R. M. Curado da Silva, et al. *IEEE Trans. on Nucl. Sci.*, 53, pp. 383-388 (2006)
5. The GRI–Gamma Ray Imager: <http://gri.cesr.fr/documents.html>;
6. R. M. Curado da Silva, et al., *SPIE Proceedings*, 4497, pp 70-78 (2002);
7. F. Lei, A. J. Dean and G. L. Hills, *Space Science Reviews*, 82, pp. 309-388 (1997);
8. R. M. Curado da Silva, et al., *IEEE Trans. Nucl. Sci.*, 50, n° 4, pag. 1198-1203 (2003);
9. E. Caroli, et al., *Nucl. Instr. and Meth. Section A*, 513, pp 350-356 (2003);
10. R.M Curado da Silva, et al., *IEEE NSS Conference Record*, 4, pp 2545 - 2550 (2007)
11. R. M. Curado da Silva, et al., *IEEE Trans. Nucl. Sci.*, 50, n° 4, pp. 1198-1203 (2003);
12. E. Caroli, et al., *Experimental Astronomy*, 20, pp 353-364, (2005)
13. G. Ventura, et al., “POLCA2 (POLarimetry with CZT Arrays): experimental set-up, calibration procedures and results” Internal Report IASF/BO n. 444/2006
14. Curado da Silva, R.M, et al., *IEEE Nuclear Science Symposium Conf. Rec.*, 2007. Volume 4, p 2545 (2007)
15. ESRF, “ID15 Handbook”, European Synchrotron Research Facility, Grenoble, (1997). Also available at the ESRF web page [www.esrf.fr/exp\\_facilities/ID15A/](http://www.esrf.fr/exp_facilities/ID15A/).